PAPER • OPEN ACCESS

Light-induced In-situ Ti^{3+} Formation in TiO$_2$ Nanosheets for Photocatalytic Hydrogen Evolution

To cite this article: E Wierzbicka *et al* 2020 *IOP Conf. Ser.: Mater. Sci. Eng.* **908** 012001

View the article online for updates and enhancements.

Light-induced In-situ Ti^{3+} Formation in TiO_2 Nanosheets for Photocatalytic Hydrogen Evolution

E Wierzbicka[1], B Osuagwu[1], N Denisov[1], D Fehn[2], K Meyer[2] and P Schmuki[1]

1 Department of Materials Science, WW4-LKO, University of Erlangen-Nuremberg, Martensstraße 7, 91058, Erlangen, Germany
2 Department of Chemistry and Pharmacy, Inorganic Chemistry, Friedrich-Alexander University Erlangen-Nürnberg (FAU), Egerlandstrasse 1, 91058 Erlangen, Germany.
E-mail: ewa.wierzbicka@fau.de

Abstract. TiO_2 has been the benchmark semiconductor for the production of photocatalytic H_2 from aqueous media (with and without sacrificial agent). On TiO_2 surfaces, the photocatalytic H_2 evolution reaction in aqueous environments is kinetically severely hampered. To overcome this limitation and reach reasonable H_2 generation rates, a well-elucidated approach is the use of noble metal co-catalysts. In contrast to costly noble metal approaches, it recently has been reported that titania reduction treatments can lead to a noble-metal-free photocatalytic H_2 generation. So-called "grey" titania due to Ti^{3+} states shows intrinsically activated photocatalytic H_2 evolution [1–3]. The present work demonstrates the feasibility to use *in-situ* photoinduced reduction to create Ti^{3+} states that act as intrinsic catalyst and activate hydrothermal synthetized anatase nanosheets for H_2 generation to mediate the transfer of photo-induced charge carriers to the electrolyte.

1. Introduction

Since the discovery of photocatalytic water splitting by Fujishima and Honda in 1972 [4], titanium dioxide has become the benchmark semiconductor for the photocatalytic production of H_2 from aqueous media (with and without sacrificial agents) [5–7]. The TiO_2 conduction band position provides the fundamental energetic precondition to produce hydrogen from pure water or alcoholic aqueous solutions, however this reaction is kinetically severely hampered [5,6,8]. Accordingly, many efforts have been made to improve the photocatalytic activity of TiO_2. The outstanding efficiency was achieved by noble metal co-catalysts deposition on TiO_2 [5,6,9,10], however the most frequently these co-catalysts are costly noble metals such as Pt, Pd or Au. More recently alternative approach has been reported that an intrinsic defect formation in titania can improve photocatalytic hydrogen generation. So-called "grey" titania obtained from pure TiO_2 by simple hydrogen annealing at elevated temperatures shows significant activation for photocatalytic H_2 evolution [3,11–13]. An observed coloration of the material is ascribed to surface defects formation (Ti^{3+}-O_v). Those defect states are able to mediate photoelectron transfer to liquid phase. Another remarkable recently reported observation is that reduced states in titania (Ti^{3+}-O_v) can be simply induced by illumination in oxygen-free water-methanol solution [14]. This finding is particularly interesting due to the simplicity of "one-pot" approach, where light firstly triggers the formation of co-catalytic defect states that then increasingly cause an enhanced H_2 evolution. Chen and Mao who first described reduced 'black' titania ascribed higher photocatalytic performance to the formation of an amorphous layer at the outer part of TiO_2 nanoparticles [15]. In our previous study on light induced formation of Ti^{3+}-O_v, the presence of amorphous layer was unclear due to high roughness of commercial anatase particles [14]. Considering above theories, herein, we investigate the photoinduced reduction to create in-situ Ti^{3+} states in hydrothermally synthetized TiO_2 nanosheets under

long time illumination (6 days). Applied hydrothermal synthesis conditions allow the formation of crystalline anatase with very well defined particles shape and sharp edges which made it possible to clearly verify if there is any change in TiO_2 surface state morphology induced by light.

2. Methodology

Anatase crystalline powder with nanosheets morphology were synthesized by a simple hydrothermal method using commercially available reagents: Tetrabutyl titanate ($Ti(OBu)_4$, Sigma Aldrich) and concentrated hydrofluoric acid (48% HF, Merck). 1.2 ml HF was added dropwise to 10 ml of $Ti(OBu)_4$ placed in a 250 ml Teflon liner, under stirring at RT. The stirring was continued for the next 40 minutes before the Teflon containing the mixture was sealed in an autoclave which was eventually transferred to a preheated oven at 200 °C. The reaction was completed after 24 h and the autoclave was allowed to cool in the oven. After hydrothermal reaction, the precipitates were collected and washed with distilled water and ethanol several times and finally dried in oven at 75 °C overnight.

The morphologies of the as-synthesized powder was characterized by a field emission scanning electron microscope (Hitachi S4800). Average particles had a size of 20-60 nm with mainly exposed [001] facets. Crystal structure of synthetized powder was investigated by XRD using an X-ray diffractometer (X'pert Philips PMD diffractometer) with a Panalytical X'celerator detector and CuKα radiation (λ=1.54056 Å). For photocatalytic H_2 evolution measurements under open circuit condition, 10 ml suspension of 2 mg powder in oxygen-free (by 30 minutes N_2 purging) water - methanol (1:1) solution was prepare in a sealed quartz tube. The suspension was continuously illuminated under a 365 nm LED (175 mW/cm^2). A gas chromatograph (GCMS-QO2010SE, SHIMADZU) with TCD detector was applied to evaluate the concentration of produced H_2. In the first cycle (24 h) of experiment, sampling was taken before and after 1. 3, 6, 9 and 24 h hours of illumination from the gas in the headspace of quartz tube. To evaluate long-term maintenance of photocatalytic activity of the powder, such cycles were repeated three times (3 x 24 h), separated by 30 minutes purge with N_2 to remove previously formed H_2 from the system.

Electron Paramagnetic Resonance (EPR) spectra were recorded on a JEOL continuous wave spectrometer JES-FA200 equipped with an Xband Gunn diode oscillator bridge, a cylindric mode cavity and a N_2 cryostat. The samples were measured in the solid state under argon atmosphere in quartz glass EPR tubes at 95 K with a similar loading of ≈ 20 mg. The EPR quartz tubes with samples and electrolyte were irradiated under LED, 365 nm, 175 mW/cm^{-2} for different time intervals. The spectra were measured with the following parameters: Temperature 95 K, microwave frequency ν = 8.959 GHz, modulation width 1.0 mT, microwave power 1.0 mW, modulation frequency 100 kHz and a time constant of 0.1 s. Data analysis and simulation was carried out using the software "eview" and "esim" written by E. Bill (MPI for Chemical Energy Conversion, Mülheim an der Ruhr).

An X-ray photoelectron spectrometer (XPS, PHI 5600 XPS spectrometer, US) was used for compositional analysis of the samples. All XPS spectra were shifted to C1s peak at 284.8 eV. All samples were transferred from reaction quartz tube to the XPS stage in an argon atmosphere. The analysis of XPS spectra was performed using Multipack software.

Transmission electron microscopy was carried out with a Philips CM30 TEM. Geometrical features were measured from TEM images using Image J software.
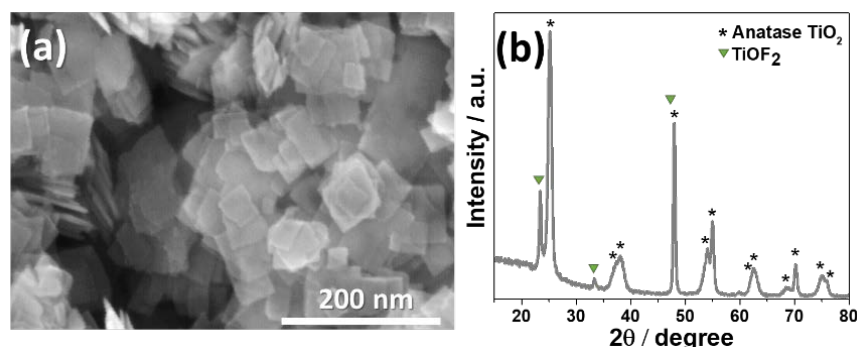
3. Results and discussion

Figure 1. (a) SEM images of as received nanosheets (powder form). (b) XRD patterns of as received powder.

Figure 1a shows the SEM images of the powder used in this study before illumination. Optimized hydrothermal synthesis conditions allow to obtain powder of nanosheets form with very well defined particles shape, sharp edges and size between 20 and 60 nm. This method of synthesis enabled morphological control to expose specific crystal facets. As received nanosheets already have crystallographic structure of anatase TiO_2 confirmed by XRD (Figure 2b), with characteristic diffraction pattern of anatase (PDF card No. 00-021-1272) and the peaks position at 25.3°, 37.8°, 38.6°, 48.0°, 53.9°, 55.1°, 62.7°, 68.8°, 70.3°, 75.0° and 76.0°. The peaks placed at 23.4°, 33.4° and 47.9° correspond to titanium oxydifluoride which is impurity from hydrothermal synthesis reaction.

The cyclic photocatalytic hydrogen evolution performance from anatase nanosheets powder under a UV light source (LED, 365 nm, 175 mW/cm^{-2}) is presented in Figure 2a. Similar to our previous studies cycling experiments show that no H_2 evolution could be detected for the first hours due to a time prerequisites for initiation of Ti^{3+}-O_v active centers. The H_2 generation have characteristic exponential growth only in the first cycle (first 24 h) [14]. Despite of illumination interruptions and nitrogen purging between the cycles, light-induced Ti^{3+}-O_v sites remain active in the following cycles. A steady, nearly linear increase of the H_2 production is observed. The average H_2 evolution rate reaches about 125 µmol h^{-1} g^{-1} in every cycle, during 3 times repeated cycles (3 x 24 h) of illumination. Notably, a change of color of the nanopowders samples can be observed during UV light exposure as shown in Figure 2b. Powders darkening is a result of light-induced formation of Ti^{3+}-O_v surface defects. It was previously shown in literature that in absence of oxygen in the reaction environment, reduction leads to the formation of color Ti^{3+} states [13,14,16]. This Ti^{3+} defects can act as an intrinsic co-catalyst for photocatalytic H_2 evolution due to their introduction create additional electronic states below the conduction band [16].

Formation of those active centers was confirmed by EPR spectroscopy (Figure 2c). For these measurements, nanosheets anatase powder slurries in O_2-free 50% methanol-waters solutions were placed in quartz EPR tubes and exposed to different illumination time with LED 365nm (175 mW/cm^2) up to 6 days (Figure 2b). The measurements of pristine TiO_2 powder (Figure 2c inset, 0 h) show a low-intensity, sharp EPR signal from naturally present Ti^{3+} defects in regular lattice position centered at $g_x = g_y = 1.99$ and one $g_z = 1.96$. Clearly, illumination (short time 3h and long time 6 days) of the nanopowders gives rise to a strong paramagnetic signature centered at a g-value of $g = 1.94$ [17] (Figure 2c) that could be fitted by the resonance of Ti^{3+} surface exposed species. Note that the signal for 6 days illumination is 10 times attenuated.
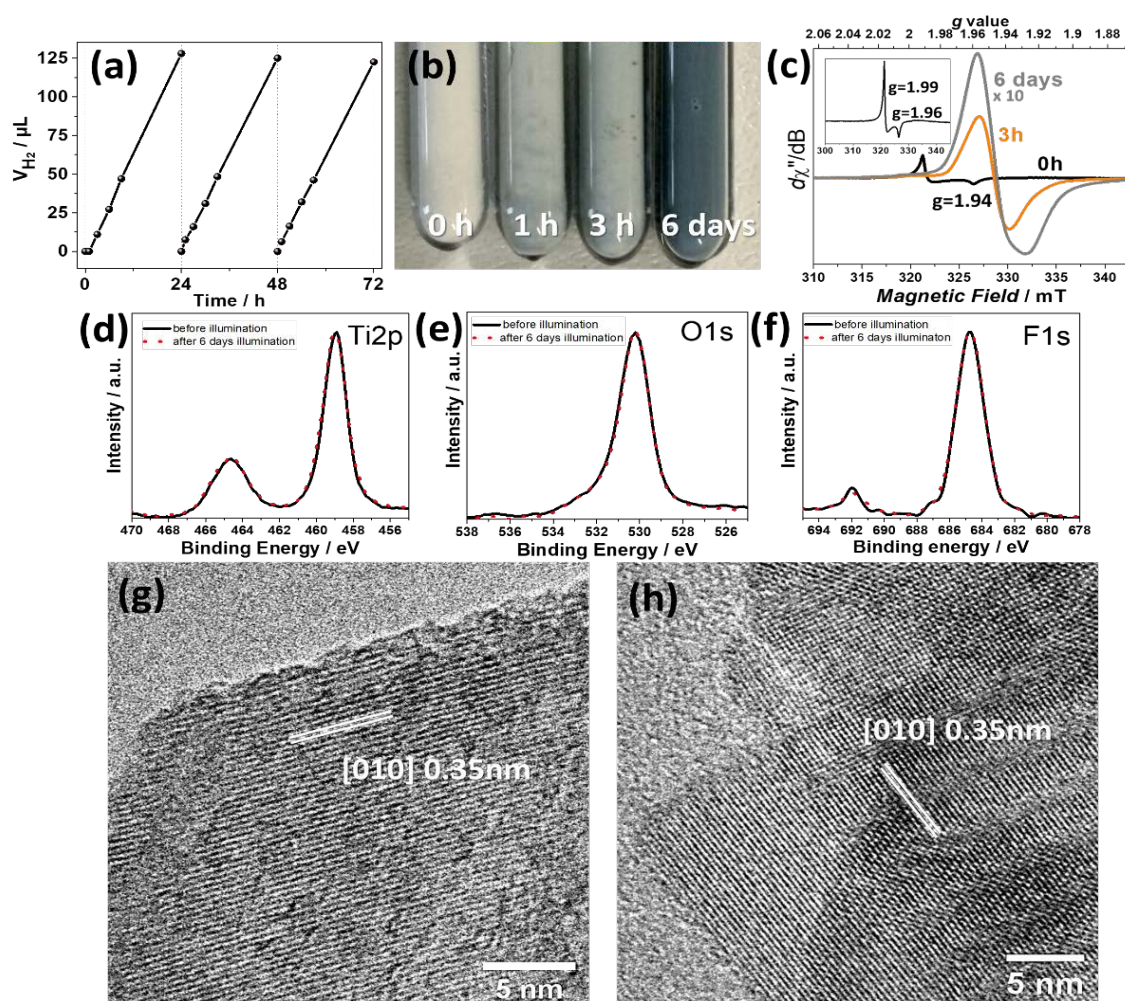
Figure 2. (a) Volume of generated H₂ on 2 mg of anatase powder (nanosheets structure) in 10 mL H₂O: methanol (50:50 vol.%) in cycling experiment under UV 365 nm light. (b) Photography illustrating changes of anatase powder (nanosheets structure) color after varied time of illumination with UV 365 nm light: (from the left side) 0 h, 1 h, 3 h and 6 days. (c) EPR spectra of the powder after varied time of illumination with UV 365 nm for 0 h, 3 h and 6 days (please note that the intensity of the sample after 6 days illumination is attenuated by a factor of 10). (d,e,f) XPS data of the powder before and after UV illumination. HR-TEM images of the nanosheets (g) before and (h) after light treatment.

The above experimental findings therefore clearly point toward a Ti^{3+}-O_v sites defect formation introduced by the illumination in anatase powder with nanosheet morphology.

The sample before and after exposure to UV light for 6 days were further studied by XPS. In the Ti2p, O1s and F1s spectra of the powders before and after illumination no changes are apparent (Figure 2d,e,f) which indicates that the concentration of Ti^{3+} states are below the XPS detection limit. Overall, HR-TEM images of the particles g) before and h) after 6 days UV illumination does not show difference in morphology (lattice fringes are evidently intact). We have identified that even long time illumination with strong UV light source (175 mW/cm^{-2}) that induced Ti^{3+}-O_v states formation [14], do not lead to amorphous shell formation. This result is in contradiction to the generally accepted theory claims that amorphous shell (large concentration of Ti^{3+}-O_v states) is necessary to form an additional mid-gap states overlapping with the conduction band edge which promote H₂ evolution, while small defect concentration leads to rapid recombination of photogenerated charge carriers. It has been proven many

times that the defect sites in the bulk of photocatalysts introduced by doping can result with recombination centres formation [18]. Our finding show that surface-localized defects like Ti^{3+}-O_v, even trace amounts, acts as metal-like co-catalyst for enhanced photocatalytic H_2 generation.

4. Conclusions

In summary, the present study demonstrates an activation of nanosheets form anatase powder for photocatalytic H_2 evolution after light-induced Ti^{3+}-O_v states formation. Particularly interesting is that the induction of Ti^{3+}-O_v defects leads to macroscopic observation of powder darkening but the defects presence is detectable only by EPR. Despite the fact that concentration of Ti^{3+}-O_v states must be extremely small, since even XPS spectra do not confirm their presence, those states are able to enhance H_2 evolution without application of any co-catalyst. Finally, application of well shaped particles in a form of nanosheets allow us to verify the lack of amorphous layer formation in the outer part of the particles. Evidently, based on presented results, even minute amount of Ti^{3+} defects, if localized on the surface of the particles, can successfully act as co-catalyst for H_2 evolution.

5. References

[1]   Liu N, Steinrück HG, Osvet A, Yang Y, Schmuki P 2017 *Appl. Phys. Lett.* **110** 072102.
[2]   Zhou X, Wierzbicka E, Liu N, Schmuki P 2019 *Chem. Commun.* **55** 533–536.
[3]   Liu N, Schneider C, Freitag D, Hartmann M, Venkatesan U, Müller J, Spiecker E, Schmuki P 2014 *Nano Lett.* **14** 3309–3313.
[4]   Fujishima A, Honda K 1972 *Nature* **238** 37–38.
[5]   Fujishima A, Rao TN, Tryk DA 2000 *J. Photochem. Photobiol. C* **1** 1–21.
[6]   Schneider J, Matsuoka M, Takeuchi M, Zhang J, Horiuchi Y, Anpo M, Bahnemann DW 2014 *Chem. Rev.* **114** 9919–9986.
[7]   De Angelis F, Di Valentin C, Fantacci S, Vittadini A, Selloni A 2014 *Chem. Rev.* **114** 9708–9753.
[8]   Linsebigler AM, Guangquan L, Yates JT 1995 *Chem. Rev.* **95** 735–758.
[9]   Ni M, Leung MKH, Leung, DYC, Sumathy K 2007 *Renew. Sustain. Energy Rev.* **11** 401–425.
[10]   Connelly K, Wahab K, Idriss H 2012 *Mater. Renew. Sustain. Energy* **1** 3.
[11]   Zhou X, Liu N, Schmidt J, Kahnt A, Osvet A, Romeis S, Zolnhofer EM, Marthala VRR, Guldi DM, Peukert W, Hartmann M, Meyer K, Schmuki P 2017 *Adv. Mater.* **29** 1604747.
[12]   Liu N, Schneider C, Freitag D, Venkatesan U, Marthala VRR, Hartmann M, Winter B, Spiecker E, Osvet A, Zolnhofer EM, Meyer K, Nakajima T, Zhou X, Schmuki P 2014 *Angew. Chem. Int. Ed.* **53** 14201–14205.
[13]   Liu N, Zhou X, Nguyen, NT, Peters K, Zoller F, Hwang I, Schneider C, Miehlich ME, Freitag D, Meyer K, Fattakhova-Rohlfing D, Schmuki P 2017 *ChemSusChem* **10** 62–67.
[14]   Wierzbicka E, Zhou X, Denisov N, Yoo JE, Fehn D, Liu N, Meyer K, Schmuki P 2019 *ChemSusChem* **12** 1900–1905.
[15]   Chen X, Liu L, Yu PY, Mao SS 2011 *Science* **331** 746–50.
[16]   Naldoni A, Allieta M, Santangelo S, Marelli M, Fabbri F, Cappelli S, Bianchi CL, Psaro R, Dal Santo V 2012 *J. Am. Chem. Soc.* **134** 7600–7603.
[17]   Naldoni A, Altomare M, Zoppellaro G, Liu N, Kment Š, Zbořil R, Schmuki P 2019 *ACS Catal.* **9** 345–364.
[18]   Ma Y, Wang X, Jia Y, Chen X, Han H, and Li C 2014 *Chem. Rev.* **114** 9987–10043.